Silicon-based electron-mediated nuclear spin quantum computer

Hsi-Sheng Goan[a] and Gerard J. Milburn[b]
Special Research Centre for Quantum Computer Technology and Department of Physics, The university of Queensland, Brisbane QLD 4072, Australia
(Version: **C**; Revised: January 25, 2000; Compiled: June 11, 2002)

We discuss the silicon-based electron-mediated nuclear spin quantum computer proposed by Kane. Basically, we reproduce the results in Kane's paper with more details and describe how single- and two-qubit operations and measurements can, in principle, be performed.

I. OUTLINE

Kane[1] proposed a scheme for implementing a quantum computer on an array of nuclear spins located on donors, phosphorus atoms ^{31}P, in silicon. In this paper we discuss this silicon-based electron-mediated nuclear spin quantum computer and reproduce mainly the results in Kane's paper with more details. In Sec. II, the basic physics of shallow donor ^{31}P, in silicon is presented. The operation conditions and energy levels calculated perturbatively for one-qubit and two-qubit systems are discussed in Sec. III, IV and VI respectively. We describe in Sec. V single-qubit rotational operations and the basic idea of the nuclear magnetic resonance (NMR). A control-not operation for the proposed quantum computer, using[2] adiabatic variations of gate voltages and a.c. magnetic field is presented in Sec. VII. We then describe a method to detect the polarization of a single nuclear spin by means of electric charge measurement in Sec. VIII. Next we discuss briefly the problem regarding the measurement process and continuous observation in Sec. IX. Issues regarding adiabatic switching for quantum gate operations are discussed in Sec. X.

II. SHALLOW DONOR IN SILICON

One of the considerations for choosing nuclear spins of ^{31}P in silicon as qubits is that $I = 1/2$ phosphorus nuclear spins are extremely well isolated from their environment. Their silicon host can in principle be purified to contain only $I = 0$ stable isotopes. The replacement of a silicon atom by a donor ^{31}P in a silicon host can occur easily since the atoms have approximately the same size. The phosphorus atom has five valence electrons. We can to first approximation assume that four of these electrons, which fill states rather similar to those of silicon, will participate in four covalent bonds with the four neighbor atoms. The extra remaining electron, at low temperature, is normally bound to the phosphorus atom which has an additional nuclear charge $+e$. Thus a P atom behaves effectively like a hydrogen-like atom embedded in silicon. One may obtain an order of magnitude estimate for the donor Bohr radius, a_B^*, and bound state energies, E_n, using the following hydrogen-like atom formula:

$$a_B^* = \epsilon \frac{m_e}{m^*} a_B, \tag{1}$$

$$E_n = \frac{m^*}{m_e} \frac{1}{\epsilon^2} E_n^H . \tag{2}$$

Given that the static dielectric constant and effective electron mass in Si: $\epsilon = 11.7$ and $m^* \approx m_T^* = 0.2 m_e$ (where m_e is the free electron mass, and m_T^* is the transverse effective mass described later), as well as the Bohr radius and bound state energies for hydrogen atom: $a_B = 0.53$Å, and $E_n^H = -13.6\text{eV}/n^2$ with n an positive integer, we obtain $a_B^* \approx 30$Å and $E_1 \approx -20$ meV. The estimated values of E_n indicate that the P donor occupies a energy level at a distance below the conduction band minimum, small compared with the (indirect) conduction-valence energy band gap ($E_g = 1.12$ eV in Si); it is thus called a shallow donor. One of the purposes of the electrons in Kane's proposed quantum computer is to mediate nuclear spin coupling. At sufficient low temperatures, electrons only occupy the lowest energy bound states ($1s$ orbitals or band) at the donors. The $1s$ electron wave function is concentrated at the donor nucleus, yielding a large hyperfine interaction energy. The estimated values of a_B^* implies that the donor electron wave function extends tens or hundreds of angstroms away from the donor nucleus, allowing electron-mediated nuclear spin coupling to occur over comparable distances.

There exists, however, more complexity in the real situation for silicon semiconductor[3]. The lowest conduction band minimum in Si is in the direction [100], and by (cubic) symmetry in other equivalent [100] directions. There are thus six conduction band minima near the zone boundaries around $|k| \sim 0.85(2\pi/a)$, where a is the lattice constant of Si. The prolate ellipsoid of constant energy near each conduction band valley has two equal transverse axes. The dispersion relation, for example, has the form

$$E(\mathbf{k}) = \frac{\hbar^2}{2}\left(\frac{k_x^2 + k_y^2}{m_T^*} + \frac{(k_z - k_{z0})^2}{m_L^*}\right) \tag{3}$$

for the ellipsoids [001] and [00$\bar{1}$], where $k_{z0} = 0.85(2\pi/a)$. There appears a longitudinal effective mass $m_L^* = 0.98\, m_e$ and transverse mass $m_T^* = 0.2\, m_e$. To obtain more precise bound state energy levels for ^{31}P donor electron in Si, one should take into account the anisotropy of the conduction band and the interaction between the six

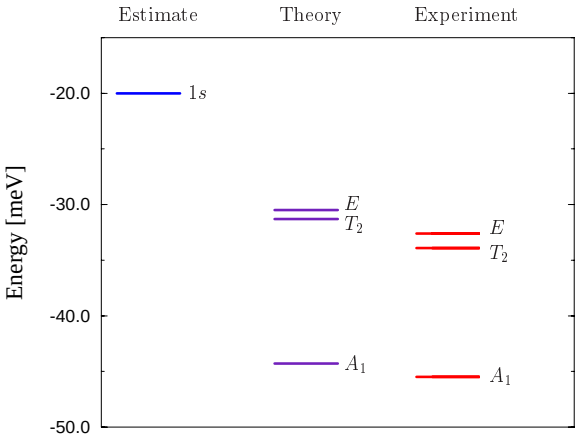

FIG. 1. Estimated value of ^{31}P $1s$ electron orbit energy in Si compared with experimental and theoretical values computed numerically by including the anisotropy of the conduction band and valley-orbit interaction in Refs.[4,5]. The valley-orbit coupling is largely responsible for the splitting of the $1s$ ground state into a singlet of A_1 symmetry, a triplet of T_2 symmetry, and a doublet of E symmetry (by using the T_d point group notation).

degenerate valleys, known as the valley-orbit coupling[3]. Fig. 1 shows the calculated and measured ^{31}P shallow donor energy levels[4,5] in Si. Note that the degeneracy of $1s$ ground states of the six equivalent [100] valleys in Si is broken in the vicinity of the donor due to the valley-orbit splitting. The shallow donor ground state[3] has an energy about -45.5 meV below the Si conduction band edge and the lowest excited state is approximately 13 meV above the ground state. This provide a condition to ignore high-lying single-electron state of the donor atom if the temperature T is such that $k_BT \ll \Delta E = 13\,\text{meV}$, where k_B is the Boltzmann constant. This condition is well satisfied, as the operation temperature, described in next section, for the proposed quantum computer is roughly at $T = 100\,\text{mK}$ ($k_BT = 0.0086\text{meV}$). Thus we may treat the effective low-energy and low-temperature Hamiltonian involving only the spin degrees of freedom of the system.

III. OPERATION CONDITIONS

We now describe the basic operation conditions for the Si:^{31}P quantum computer system. Throughout the computation the electrons must be in a non-degenerate ground state to avoid irreversible interactions between electron and nuclear spins occurring as the computation proceeds. An external magnet field, $\mathbf{B}$, is applied to break the shallow donor electron ground state two-fold spin degeneracy. At sufficient low temperature T, the electron will only occupy the lowest energy spin level when the electron Zeeman splitting is much larger than the thermal energy, $g_e\mu_B B \gg k_BT$, where μ_B is the Bohr magneton, and $g_e \approx 2$ is the Lande g-factor in Si. At $T = 100$mK and $B = 2$ tesla ($2\mu_B B = 0.23$meV), the electrons will be completely spin-polarized:

$$\frac{n^e_\uparrow}{n^e_\downarrow} \approx \exp[-2\mu_B B/(k_BT)] \approx 2.14 \times 10^{-12}, \tag{4}$$

where n^e represents the donor electron number density. These conditions however do not fully polarize the nuclear spins:

$$\frac{n^n_\downarrow}{n^n_\uparrow} \approx \exp[-2g_n\mu_n B/(k_BT)] \approx 0.98, \tag{5}$$

where n^n stands for the donor nuclear number density, the nuclear g-factor $g_n = 1.13$ for ^{31}P, μ_n is the nuclear magneton and $2g_n\mu_n B \approx 0.00014$ meV. The polarizations of the nuclear spins are instead determined by interactions with the polarized electrons.

In Table I, we list some relevant and typical energy scales in mini electron Volts (meV) and their corresponding frequencies in Hertzes (Hz) for the silicon-based electron-mediated nuclear spin quantum computer.

IV. SINGLE-QUBIT SYSTEM

The effective low-energy and low-temperature Hamiltonian for a ^{31}P nuclear spin-electron system in Si with $B \parallel z$ can be written as

$$\mathcal{H}_{en} = \mu_B B\sigma^e_z - g_n\mu_n B\sigma^n_z + A\boldsymbol{\sigma}^e \cdot \boldsymbol{\sigma}^n, \tag{6}$$

where e and n appearing in the superscripts and subscripts represent quantities for the electron and the nucleus respectively, σ's are Pauli matrices, and $A = 8\pi\mu_B g_n\mu_n|\Psi(0)|^2/3$ is the contact hyperfine interaction energy with $|\Psi(0)|^2$ the probability density of the electron wave function evaluated at the position of the nucleus. Direct diagonization of this simple Hamiltonian Eq. (6) gives the eigen energies, with each associated eigen state as a subscript (e.g., $E_{|en\rangle}$ stands for the energy of the state $|en\rangle$), as follows:

$$E_{|\uparrow 0\rangle} = \mu_B B - g_n\mu_n B + A, \tag{7}$$

$$E_{\alpha|\uparrow 1\rangle+\gamma|\downarrow 0\rangle} = \sqrt{(\mu_B B + g_n\mu_n B)^2 + (2A)^2} - A, \tag{8}$$

$$E_{-\gamma|\uparrow 1\rangle+\alpha|\downarrow 0\rangle} = -\sqrt{(\mu_B B + g_n\mu_n B)^2 + (2A)^2} - A, \tag{9}$$

$$E_{|\downarrow 1\rangle} = -\mu_B B + g_n\mu_n B + A. \tag{10}$$

Here the eigen states are written in electron σ^e_z and nuclear σ^n_z basis. For example, $|e\,n\rangle = |\downarrow 0\rangle$ represents the electron spin down ($\downarrow$) and nuclear spin up (0) state. The coefficients α and γ are:

energy	meV	Hz
indirect conduction-valence energy band gap E_g of Si	1120	2.7×10^{17}
electron ground state energy of ^{31}P donor in Si	-45.5	1.1×10^{13}
electron 1st excited state energy of ^{31}P donor in Si	-33.9	8.2×10^{12}
2nd electron binding energy in D^- state of ^{31}P donor in Si	1.7	4.1×10^{11}
temperature energy scale k_BT at $T = 100$ mK	0.0086	2.1×10^{9}
electron Zeeman energy $\mu_B B$ at $B = 2$T	0.116	2.8×10^{10}
nuclear Zeeman energy $g_n\mu_n B$ at $B = 2$T	7.1×10^{-5}	1.7×10^{7}
*typical hyperfine interaction A	1.2×10^{-4}	2.9×10^{7}
*typical nuclear resonance energy $h\nu_A$ for single qubit	3.8×10^{-4}	9.3×10^{7}
nuclear full width at half maxima $4g_n\mu_n B_{ac}$ at $B_{ac} = 10^{-3}$T	1.4×10^{-7}	3.4×10^{4}
*typical electron exchange energy $4J$	0.124	3.0×10^{10}
*typical nuclear exchange energy $h\nu_J$	3.1×10^{-7}	7.5×10^{4}

TABLE I. Relevant energy scales for the silicon-based electron-mediated nuclear spin quantum computer proposed by Kane. Here * represents that these energies can be controlled externally by varying the A-gate and J-gate voltages.

$$\alpha = \left[1 + \left(\Lambda - \sqrt{1+\Lambda^2}\right)^2\right]^{-1/2}, \tag{11}$$

$$\gamma = \left[1 + \left(\Lambda + \sqrt{1+\Lambda^2}\right)^2\right]^{-1/2}, \tag{12}$$

where $\Lambda = (\mu_B B + g_n\mu_n B)/(2A)$. We can see that if Λ is very large, which is usually the case for the proposed quantum computer, then $\alpha \to 1$ and $\gamma \to 0$.

For the sake of the more complicated two-qubit Hamiltonian encountered later, let us nevertheless calculate the energy levels perturbatively, by treating the hyperfine interaction, A, as a perturbation. The standard perturbation theory gives the first and second order energy shifts to the state $|n\rangle$ with energy level $E_n^{(0)}$ as follows:

$$E_n^{(1)} = \langle n|\mathcal{H}'|n\rangle, \tag{13}$$

$$E_n^{(2)} = \sum_{m\neq n} \frac{\langle n|\mathcal{H}'|m\rangle\langle m|\mathcal{H}'|n\rangle}{E_n^{(0)} - E_m^{(0)}}. \tag{14}$$

where $\mathcal{H}'$ is the Hamiltonian of the perturbation. The expectation values of $\mathcal{H}' = A\boldsymbol{\sigma}^e \cdot \boldsymbol{\sigma}^n$ with respect to the unperturbed states ($|\uparrow 0\rangle$, $|\downarrow 1\rangle$, $|\uparrow 1\rangle$, and $|\downarrow 0\rangle$) give the first order energy shifts of A to $|\uparrow 0\rangle$ and $|\downarrow 1\rangle$ states, and energy shifts of $-A$ to $|\uparrow 1\rangle$ and $|\downarrow 0\rangle$ states. To obtain the second-order energy shift for a state, we should find all non-zero matrix elements of $\mathcal{H}'$ connected to that state. The only non-zero matrix elements relevant for the second order perturbation energy shift are $\langle\uparrow 1|\mathcal{H}'|\downarrow 0\rangle = \langle\downarrow 0|\mathcal{H}'|\uparrow 1\rangle = 2A$. Therefore by means of Eq. (14), the energy levels to the second order in A are given by:

$$E^{(2)}_{|\uparrow 0\rangle} = \mu_B B - g_n\mu_n B + A, \tag{15}$$

$$E^{(2)}_{|\uparrow 1\rangle} = \mu_B B + g_n\mu_n B - A + \frac{2A^2}{\mu_B B + g_n\mu_n B}, \tag{16}$$

$$E^{(2)}_{|\downarrow 1\rangle} = -\mu_B B + g_n\mu_n B + A, \tag{17}$$

$$E^{(2)}_{|\downarrow 0\rangle} = -\mu_B B - g_n\mu_n B - A - \frac{2A^2}{\mu_B B + g_n\mu_n B}. \tag{18}$$

If the electron is in its spin-down polarized ground state, the frequency separation between the two associated energy levels, Eq. (17) and (18), is found to be

$$h\nu_A = 2g_n\mu_n B + 2A + \frac{2A^2}{\mu_B B}, \tag{19}$$

where the nuclear Zeeman energy $g_n\mu_n B$ has been neglected with respect to the electron Zeeman energy $\mu_B B$ in the denominator of the last term of Eq. (19). Eqs. (15) – (19) can also be obtained to the second order in A by directly expanding the exact eigen energies, Eqs. (7) – (10), up to the second power of Λ^{-1}. In addition, the coefficients of the states, also by direct expansion of Eqs. (11) and (12) to the first power of Λ^{-1} and by using the relation $\alpha^2 + \gamma^2 = 1$, have the approximate values:

$$\alpha = \left[1 - \left(\frac{A}{\mu_B B + g_n\mu_n B}\right)^2\right]^{\frac{1}{2}}, \tag{20}$$

$$\gamma = \frac{A}{\mu_B B + g_n\mu_n B}. \tag{21}$$

This result can be obtained by calculating the first-order wave function shift using the perturbation theory. In a Si:^{31}P system, $2A/h = 58$MHz, and $A > g_n\mu_n B$ for $B < 3.5$T.

Applying the A-gate voltage (on the top of the donor atom, see Fig. 7) shifts electron wave function envelope away from the nucleus and reduces the hyperfine interaction. To get an order of magnitude estimate for the size of this shift, we assume a linear decrease of A with increasing voltage, i.e., $A \to A - \eta V$ with a tuning parameter $\eta = 30\,$MHz/V. The corresponding estimated nuclear resonance frequency change, following from Eq. (19), as a function of applied voltage with the assumed linear tuning parameter is shown in Fig. 2. This crude estimate gives roughly the nuclear resonance frequency change for the curve shown in Fig. 2 in Kane's paper[1].

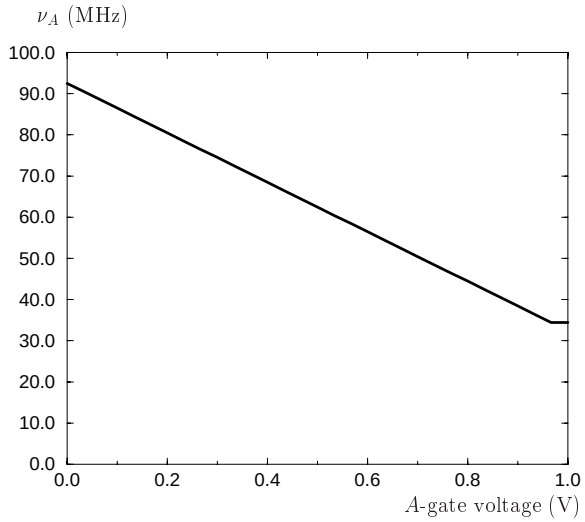

FIG. 2. Estimate of nuclear resonance frequency, ν_A, as a function of applied A-gate voltage with the assumed linear tuning parameter $\eta = 30\,\mathrm{MHz/V}$.

V. SINGLE-QUBIT OPERATIONS: NUCLEAR MAGNETIC RESONANCE

Since the nuclear resonance frequency is controllable externally, the nuclear spins can be selectively brought into resonance with a globally applied a.c. magnetic field, B_{ac}, allowing arbitrary rotations to be performed on each nuclear spin. Let us discuss briefly this nuclear magnetic resonance (NMR) technique. For simplicity, we consider first the Hamiltonian for a free nuclear spin-$\frac{1}{2}$ system with a uniform magnetic field, B, applied in the z-direction, and an a.c. magnetic field rotating in the xy-plane:

$$\mathcal{H}_{NMR} = -g_n\mu_n B\sigma_z^n - g_n\mu_n B_{ac}[\sigma_x^n\,\cos(\omega t) + \sigma_y^n \sin(\omega t)]. \tag{22}$$

An exact solution for this problem is available. Let $P_{|1\rangle}$ and $P_{|0\rangle}$ be the probabilities of finding the nuclear spin in the down ($|1\rangle$) and up ($|0\rangle$) states respectively. If initially, at $t = 0$, $P_{|0\rangle} = 1$ and $P_{|1\rangle} = 0$, then at time t, the probability for being found in each of the two states is given by the so-called Rabi's formula:

$$P_{|1\rangle}(t) = \frac{(g_n\mu_n B_{ac}/\hbar)^2}{(g_n\mu_n B_{ac}/\hbar)^2 + (\omega-\omega_{10})^2/4} \times \sin^2\left[\left(\frac{(g_n\mu_n B_{ac})^2}{\hbar^2} + \frac{(\omega-\omega_{10})^2}{4}\right)^{\frac{1}{2}} t\right], \tag{23}$$

$$P_{|0\rangle}(t) = 1 - P_{|1\rangle}(t), \tag{24}$$

where

$$\omega_{10} = (E_{|1\rangle} - E_{|0\rangle})/\hbar = 2g_n\mu_n B/\hbar \tag{25}$$

is the angular frequency separation between the two states, $|1\rangle|$ and $0\rangle$, connected by the B_{ac}, which is equal to the nuclear spin-precession frequency for the $B \neq 0$, $B_{ac} = 0$ problem. The amplitude of the oscillatory spin-flop probability $P_{|1\rangle}(t)$ is particularly large when the frequency of the rotating magnetic field coincides with the frequency separation between the two states:

$$\omega = \omega_{\mathrm{res}} = \omega_{10}. \tag{26}$$

Eq. (26) is therefore known as the resonance condition. The full width at half maxima of the amplitude in frequency, $(\Delta\omega)_\Gamma$, is given by

$$(\Delta\omega)_\Gamma = 4g_n\mu_n B_{ac}/\hbar. \tag{27}$$

It is worth noting that the weaker the a.c. magnetic field B_{ac}, the narrower the resonance profile. Next we describe briefly what happens to the corresponding state vector, $|\psi(t)\rangle$, at resonance $\omega = \omega_{10}$. If the time-evolution state is written as:

$$|\psi(t)\rangle = a(t)|0\rangle + b(t)|1\rangle, \tag{28}$$

the time-dependent coefficients at resonance, $\omega = \omega_{10}$, can be obtained as:

$$a(t) = \exp(-i\omega t)\cos\left(\frac{g_n\mu_n B_{ac}}{\hbar}t\right), \tag{29}$$

$$b(t) = i\,\exp(i\omega t)\sin\left(\frac{g_n\mu_n B_{ac}}{\hbar}t\right). \tag{30}$$

A $(g_n\mu_n B_{ac}t_\pi)/\hbar = \pi$ pulse then causes the expectation value of the magnetization vector to undergo a rotation and return to its initial value.

In practice, a rotating magnetic field may be difficult to produce experimentally. A horizontally oscillating magnetic field linearly polarized along, for example, in the x-direction is usually applied. This oscillating magnetic field can be decomposed into a counterclockwise rotating field component and a clockwise component as follows:

$$B_{ac}\,\hat{\mathbf{x}}\cos(\omega t) = \frac{B_{ac}}{2}[\hat{\mathbf{x}}\cos(\omega t) + \hat{\mathbf{y}}\sin(\omega t)] + \frac{B_{ac}}{2}[\hat{\mathbf{x}}\cos(\omega t) - \hat{\mathbf{y}}\sin(\omega t)]. \tag{31}$$

The effect of the clockwise component can be obtained simply by reversing the sign of ω for the counterclockwise component. Suppose the resonance condition is met for the counterclockwise component, $\omega = \omega_{10} = 2g_n\mu_n B/\hbar$. The experimental operation conditions for magnetic fields ($B = 2\mathrm{T}$ and $B_{ac} = 10^{-3}\mathrm{T}$), i.e.,

$$\frac{B_{ac}}{B} = 5\times 10^{-4} \ll 1, \tag{32}$$

imply that the full width at half maxima in frequency, Eq. (27), of the probability amplitude, Eq. (23), is much smaller than the resonance frequency:

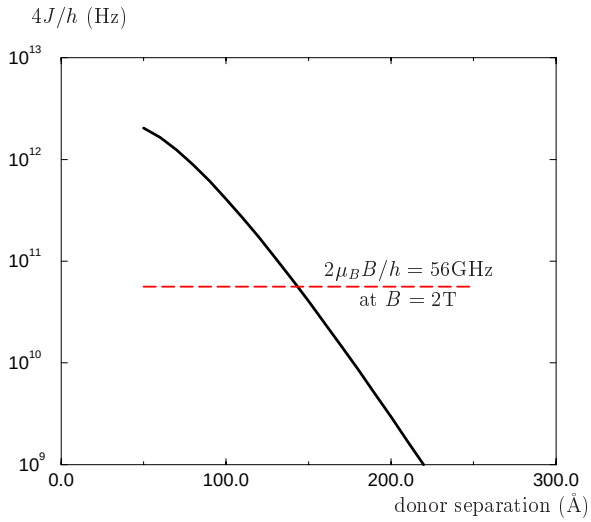

FIG. 3. Exchange frequency $4J(r)/h$ as a function of separation distance between donors.

$$(\Delta\omega)_\Gamma \ll \omega = \omega_{\rm res} = \omega_{10}. \tag{33}$$

Since the effect of the clockwise component amounts to $\omega \to -\omega$, which is far outside the resonance peak, the amplitude in this case becomes small in magnitude as well as very rapidly oscillating. As a result, whenever the resonance condition is met for the counterclockwise component, the effect of the clockwise component becomes completely negligible. Hence, for the linearly polarized oscillating magnetic field, Eq. (31), if $|\omega| = |\omega_{\rm res}|$, one of the two rotating field components has the right sense of rotation.

As to the case for the single-qubit rotational operations, if the resonance frequency is tuned to the separation frequency between $|\downarrow 1\rangle$ and $|\downarrow 0\rangle$ states, given by Eq. (19), and the temperature is low enough, we may, to an approximation, consider only the polarized electron ground state subspace. In this case, the above NMR description for a free nuclear spin-$\frac{1}{2}$ system can be well applied to the single-qubit system with some suitable changes of parameters.

VI. TWO-QUBIT SYSTEM

The effective Hamiltonian for two coupled donor nuclear spin-electron systems, valid at energy scales small compared to the donor-electron binding energy, is

$$\begin{aligned}\mathcal{H}_{coup} = \mu_B B\sigma_z^{1e} - g_n\mu_n B\sigma_z^{1n} + \mu_B B\sigma_z^{2e} - g_n\mu_n B\sigma_z^{2n} \\ + A_1\boldsymbol{\sigma}^{1e}\cdot\boldsymbol{\sigma}^{1n} + A_2\boldsymbol{\sigma}^{2e}\cdot\boldsymbol{\sigma}^{2n} + J\boldsymbol{\sigma}^{1e}\cdot\boldsymbol{\sigma}^{2e},\end{aligned} \tag{34}$$

where A_1 and A_2 are the hyperfine interaction energies of the respective nucleus-electron systems and $4J$, the exchange energy, depends on the overlap of the electron wave functions. In order for exchange coupling between the electron spins to be significant, the separation between donors should not be too large. As shall be seen below, significant coupling between nuclei will occur when $4J \approx 2\mu_B B$. This condition sets an approximately necessary separation between donors. To get an estimate about the necessary separation, let us use the formula for exchange interaction, derived for well separated H-H atoms but with values appropriate for ^{31}P donors in Si:

$$4J(r) \approx 1.6\frac{e^2}{\epsilon a_B^*}\left(\frac{r}{a_B^*}\right)^{5/2}\exp\left(-\frac{2r}{a_B^*}\right), \tag{35}$$

where r is the distance between donors. This exchange energy with the static dielectric constant $\epsilon = 11.7$ and donor Bohr radius $a_B^* \approx 30$Å, employed before, is plotted in Fig. 3. One can see that when $4J \approx 2\mu_B B = 56$GHZ, the separation between donors is roughly located in $100 - 200$Å. Since the value of J depends on the electron wave function overlap, it can be varied by an J-gate positioned between the donors (see Fig. 7). The actual necessary separation between donors may be thus a little larger than 200Å. In practice, the exchange interaction is complicated in Si because the contribution from each valley interferes, leading to oscillatory behavior[6] of $J(r)$.

Next we describe the energy levels of Hamiltonian for two coupled donor nuclear spin-electron systems, Eq. (34), as a function of J. Let us first consider only the electrons. If $B = 0$, only the exchange interaction left in the Hamiltonian and it can be rewritten as:

$$\begin{aligned}J\boldsymbol{\sigma}^{1e}\cdot\boldsymbol{\sigma}^{2e} &= 4J\,\mathbf{S}_{1e}\cdot\mathbf{S}_{2e} = 2J(\mathbf{S}^2 - \mathbf{S}_{1e}^2 - \mathbf{S}_{2e}^2) \\ &= \begin{cases} J & : \quad S = 1 \\ -3J & : \quad S = 0 \end{cases},\end{aligned} \tag{36}$$

where $\mathbf{S}_{ie}$, individual electron spin-$\frac{1}{2}$ operator, satisfies $\mathbf{S}_{ie}^2 = S_{ie}(S_{ie}+1) = 3/4$, $\mathbf{S}$ is the total spin operator of the two electrons and $\mathbf{S}^2$ has eigenvalue $S(S+1)$ in states of total spin S. The exchange interaction lowers the total electron spin $S = 0$ singlet $(|\uparrow\downarrow\rangle - |\downarrow\uparrow\rangle)/\sqrt{2}$ energy with respect to the $S = 1$ triplet, $|\uparrow\uparrow\rangle$, $(|\uparrow\downarrow\rangle + |\downarrow\uparrow\rangle)/\sqrt{2}$, $|\downarrow\downarrow\rangle$, by the triplet-singlet splitting $4J$, i.e., $E_s = -3J$ and $E_t = J$. Suppose now the B field is turned on, the magnetic field causes the Zeeman splitting of $\pm 2\mu_B B$ on $|\uparrow\uparrow\rangle$ and $|\downarrow\downarrow\rangle$ states but has no effect on the states $(|\uparrow\downarrow\rangle \pm |\downarrow\uparrow\rangle)/\sqrt{2}$ since their z-components of the total two-electron spins are zeros. If J is adiabatically increased, the energy levels of $|\downarrow\downarrow\rangle$ and $(|\uparrow\downarrow\rangle - |\downarrow\uparrow\rangle)/\sqrt{2}$ states cross each other at the point where the triplet-singlet splitting is equal to the Zeeman splitting $4J = 2\mu_B B$, and the $(|\uparrow\downarrow\rangle - |\downarrow\uparrow\rangle)/\sqrt{2}$ state has the lowest energy when $J > \mu_B B/2$ (see Fig. 4).

Now let us add back the nuclear spins to the Hamiltonian. Generally the nuclear energy splitting is much smaller than electron one by a factor of about $\mu_B/\mu_n \approx 1800$. It is hence hard to draw the whole electron and nuclear energy levels to the same scale. Nevertheless in the case when nuclear spins are included, each widely spaced electron energy level will become four

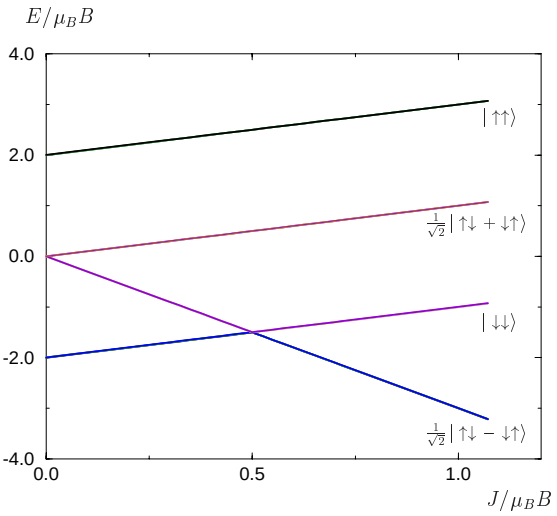

FIG. 4. Energy levels of two-qubit system as a function of exchange energy J.

much closer electron-nuclear energy levels and there are sixteen electron-nuclear spin states in total (see Fig. 4). In a magnetic field, the $|\downarrow\downarrow\rangle$ state will be the electron ground state if $k_BT \ll J < \mu_B B/2$. In the polarized $|\downarrow\downarrow\rangle$ electron states, the energies of the nuclear states can be calculated to the second order in A using the perturbation theory. We diagonalize the unperturbed Hamiltonian and then find the non-zero matrix elements of the perturbation,

$$\mathcal{H}' = A_1 \boldsymbol{\sigma}^{1e} \cdot \boldsymbol{\sigma}^{1n} + A_2 \boldsymbol{\sigma}^{2e} \cdot \boldsymbol{\sigma}^{2n}, \tag{37}$$

with respect to the unperturbed eigen states. Let us introduce the following notations for the electron and nuclear states for abbreviation:

$$|s_e\rangle = \frac{1}{\sqrt{2}}|\uparrow\downarrow + \downarrow\uparrow\rangle, \tag{38}$$

$$|a_e\rangle = \frac{1}{\sqrt{2}}|\uparrow\downarrow - \downarrow\uparrow\rangle, \tag{39}$$

$$|s_n\rangle = \frac{1}{\sqrt{2}}|10 + 01\rangle, \tag{40}$$

$$|a_n\rangle = \frac{1}{\sqrt{2}}|10 - 01\rangle. \tag{41}$$

We focus on the nuclear spin energy levels in the spin-polarized electron ground states. These unperturbed energy levels and states in are:

$$E^{(0)}_{|\downarrow\downarrow\rangle|11\rangle} = -2\mu_B B + 2g_n\mu_n B + J, \tag{42}$$

$$E^{(0)}_{|\downarrow\downarrow\rangle|s_n\rangle} = -2\mu_B B + J, \tag{43}$$

$$E^{(0)}_{|\downarrow\downarrow\rangle|a_n\rangle} = -2\mu_B B + J, \tag{44}$$

$$E^{(0)}_{|\downarrow\downarrow\rangle|00\rangle} = -2\mu_B B - 2g_n\mu_n B + J. \tag{45}$$

For simplicity, let us consider the case where $A_1 = A_2 = A$ in $\mathcal{H}'$, Eq. (37). To obtain the first-order energy shift, it is sufficient to evaluate the expectation value of $\mathcal{H}'$ with respect to the unperturbed states. The first-order energy shifts of $|\downarrow\downarrow\rangle|11\rangle$ and $|\downarrow\downarrow\rangle|00\rangle$ are $2A$ and $-2A$ respectively. The $|\downarrow\downarrow\rangle|s_n\rangle$ and $|\downarrow\downarrow\rangle|a_n\rangle$ states, however, remain degenerate since there is no first-order energy shift to both of them. The only non-zero matrix elements connected to the above four electron-nuclear spin states by $\mathcal{H}'$, Eq. (37), relevant to the second-order energy shifts are:

$$\langle s_e|\langle 11|\mathcal{H}'|\downarrow\downarrow\rangle|s_n\rangle = 2A, \tag{46}$$

$$\langle a_e|\langle 11|\mathcal{H}'|\downarrow\downarrow\rangle|a_n\rangle = -2A, \tag{47}$$

$$\langle s_e|\langle s_n|\mathcal{H}'|\downarrow\downarrow\rangle|00\rangle = 2A, \tag{48}$$

$$\langle a_e|\langle a_n|\mathcal{H}'|\downarrow\downarrow\rangle|00\rangle = 2A. \tag{49}$$

Their complex conjugates, which are equal to themselves, are not shown here. Other relevant unperturbed energy levels associated with states in Eq. (46)–(49) are given by:

$$E^{(0)}_{|s_e\rangle|11\rangle} = 2g_n\mu_n B + J, \tag{50}$$

$$E^{(0)}_{|a_e\rangle|11\rangle} = 2g_n\mu_n B - 3J, \tag{51}$$

$$E^{(0)}_{|s_e\rangle|s_n\rangle} = J, \tag{52}$$

$$E^{(0)}_{|a_e\rangle|a_n\rangle} = -3J. \tag{53}$$

Using the second-order energy shift formula, Eq. (14), we find that the electron-nuclear spin energy levels in the electron spin-polarized $|\downarrow\downarrow\rangle$ states, to the second order in A, are:

$$E^{(2)}_{|\downarrow\downarrow\rangle|11\rangle} = -2\mu_B B + 2g_n\mu_n B + J + 2A, \tag{54}$$

$$E^{(2)}_{|\downarrow\downarrow\rangle|s_n\rangle} = -2\mu_B B + J - \frac{2A^2}{\mu_B B + g_n\mu_n B}, \tag{55}$$

$$E^{(2)}_{|\downarrow\downarrow\rangle|a_n\rangle} = -2\mu_B B + J - \frac{2A^2}{\mu_B B + g_n\mu_n B - 2J}, \tag{56}$$

$$E^{(2)}_{|\downarrow\downarrow\rangle|00\rangle} = -2\mu_B B - 2g_n\mu_n B + J - 2A - \frac{2A^2}{\mu_B B + g_n\mu_n B} - \frac{2A^2}{\mu_B B + g_n\mu_n B - 2J}. \tag{57}$$

The $|\downarrow\downarrow\rangle|a_n\rangle$ state is lowered in energy with respect to $|\downarrow\downarrow\rangle|s_n\rangle$ by:

$$h\nu_J = 2A^2\left(\frac{1}{\mu_B B - 2J} - \frac{1}{\mu_B B}\right). \tag{58}$$

The $|\downarrow\downarrow\rangle|11\rangle$ state is above the $|\downarrow\downarrow\rangle|s_n\rangle$ state and the $|\downarrow\downarrow\rangle|00\rangle$ state below the $|\downarrow\downarrow\rangle|a_n\rangle$ state by an energy $h\nu_A$, Eq. (19). For the Si:^{31}P system at $B = 2$T and for $4J/h = 30$GHz, Eq. (58) yields the effective nuclear exchange frequency $\nu_J \approx 75$ KHz. This nuclear spin exchange frequency approximates the rate at which binary operations can be performed on the computer (see the discussion in Sec. X).

VII. CONTROLLED-NOT OPERATION

The controlled-NOT operation (conditional rotation of the target spin by 180°) can be realized[2] by the combined applications of B_{ac} and adiabatic variations in J and $\Delta A = A_1 - A_2$, in which the gate biases are varied slowly. The sequence of the adiabatic steps performed and the associated evolution of nuclear spin states and energy levels for the controlled-NOT operation are schematically illustrated in Fig. 5. Issues regarding adiabatic processes, such as adiabatic switching times and pulse shapes are discussed in Sec. X.

At $t = t_0$, indicated in Fig. 5 , the two spin systems are uncoupled (J=0) and $\Delta A = 0$ so that $|10\rangle$ and $|01\rangle$ are degenerate. At t_1, $\Delta A > 0$ ($A_1 > A_2$) breaks this degeneracy ($|10\rangle$ above $|01\rangle$) and distinguishes the control qubit from the target qubit. At t_2, J is turned on and in the case when $\Delta A \gg h\nu_J$, the eigenstates do not evolve away from themselves much, i.e., they roughly remain in the same states as they were. When ΔA is slowly decreased to zero with J on, the $|10\rangle$ state evolves adiabatically into $|s_n\rangle$ state and $|01\rangle$ into $|a_n\rangle$. The energy splitting between the central levels at t_3 then reduce to the effective nuclear spin exchange frequency $h\nu_J$ between $|s_n\rangle$ and $|a_n\rangle$ states. At t_4, a linear polarized magnetic field B_{ac} is applied, for example, in the x-direction resonant with the $|11\rangle$ — $|s_n\rangle$ gap. At first sight, B_{ac} seems to be also resonant with the $|00\rangle$ — $|a_n\rangle$ gap; however, to the first order in time-dependent perturbation theory, the matrix element of this transition is zero since the nuclear singlet state is not coupled to the other triplet states by the perturbation:

$$g_n\mu_n(\sigma_x^{1n} + \sigma_x^{2n})B_{ac}\cos(\omega t). \tag{59}$$

B_{ac} is left on until t_5, when it has transformed $|11\rangle$ into $|s_n\rangle$ and vice versa. The $|s_n\rangle$ and $|a_n\rangle$ states are then adiabatically transformed back into $|10\rangle$ and $|01\rangle$ in a reverse of the sequence of steps performed at the beginning of the operation.

We can see that the qubits whose energy levels vary during the adiabatic procedure are unchanged. However, the states are inverted if and only if the control qubit (first qubit) is $|1\rangle$. Therefore the controlled-NOT operation has been performed.

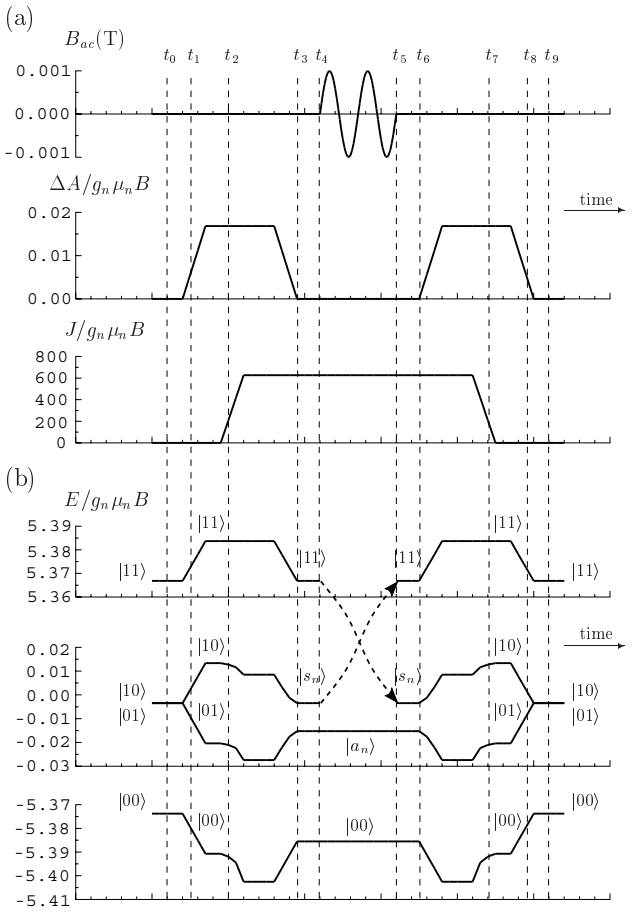

FIG. 5. The controlled-NOT operation realized by the combined applications of B_{ac} and adiabatic variations in J and $\Delta A = A_1 - A_2$. (a) The sequence of controls are illustrated schematically. All energy scales are in units of nuclear Zeeman energy: $g_n\mu_n B$. (b) The corresponding evolution of the nuclear spin states and energy levels are presented. Throughout the controlled-NOT operation $J < \mu_B B/2$. As a consequence, the electron spin state of the system is always in polarized $|\downarrow\downarrow\rangle$ state and only the associated nuclear spin states are explicitly shown. Note that the energy levels are presented at the same scale but in different energy intervals, and they are obtained by keeping $A_2 \approx 1.683\, g_n\mu_n B \approx 0.001\,\mu_B B$ fixed and varying $A_1 = A_2 + \Delta A$.

VIII. SPIN MEASUREMENTS

The computations of the proposed quantum computer are done when $J < \mu_B B/2$ where the electrons are fully polarized. Measurements are, however, made when $J > \mu_B B/2$ where electron $|a_e\rangle$ states have the lowest energies (Fig. 4). As the electron levels cross (see Fig. 4), the $|\downarrow\downarrow\rangle$ and $|a_e\rangle$ states are coupled by hyperfine interactions, Eq. (37), with the nuclei. The no-level crossing theorem in quantum mechanics states that a pair of energy levels connected by perturbation do not cross

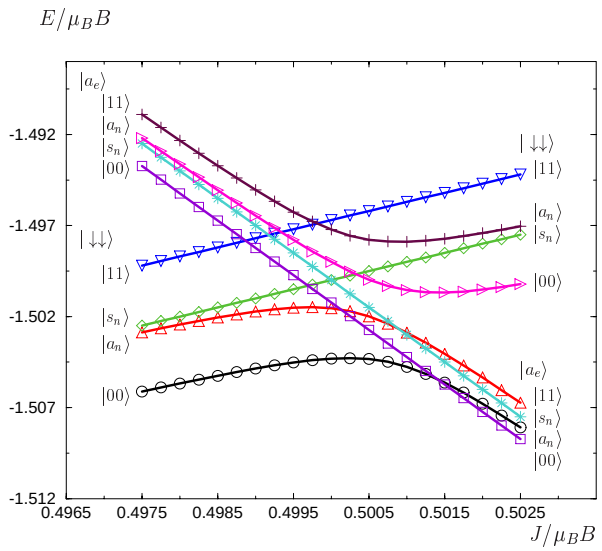

FIG. 6. Adiabatic evolution of the lowest eight energy states in the vicinity of $J = \mu_B B/2$ with $A_1 = A_2 \approx 0.001\,\mu_B B$.

as the strength of the perturbation is varied. We see from Eq. (46) – (49) that for the lowest eight energy states, only two pairs of states are connected by hyperfine interactions, Eq. (37), as the exchange energy J is varied. The first pair of states consists of $|\downarrow\downarrow\rangle|a_n\rangle$ and $|a_e\rangle|11\rangle$, and the members of the other pair are $|\downarrow\downarrow\rangle|00\rangle$ and $|a_e\rangle|a_n\rangle$ states. The coupled states in each pair hybridize and their energy levels repel each other, leading to anti-crossing behavior in the vicinity of $J = \mu_B B/2$, shown in Fig. 6. Other energy levels, however, do cross each other since no coupling exists between them. Thus during an adiabatic increase in J (from $J < \mu_B B/2$ to $J > \mu_B B/2$), the lowest eight states evolve, as illustrated in Fig. 6, as follows:

$$\begin{aligned}
|a_e\rangle|11\rangle &\longrightarrow |\downarrow\downarrow\rangle|a_n\rangle,\\
|a_e\rangle|a_n\rangle &\longrightarrow |\downarrow\downarrow\rangle|00\rangle,\\
|a_e\rangle|s_n\rangle &\longrightarrow |a_e\rangle|s_n\rangle,\\
|a_e\rangle|00\rangle &\longrightarrow |a_e\rangle|00\rangle,\\
|\downarrow\downarrow\rangle|11\rangle &\longrightarrow |\downarrow\downarrow\rangle|11\rangle,\\
|\downarrow\downarrow\rangle|s_n\rangle &\longrightarrow |\downarrow\downarrow\rangle|s_n\rangle,\\
|\downarrow\downarrow\rangle|a_n\rangle &\longrightarrow |a_e\rangle|11\rangle,\\
|\downarrow\downarrow\rangle|00\rangle &\longrightarrow |a_e\rangle|a_n\rangle.
\end{aligned} \tag{60}$$

We now describe how the polarization of a single ^{31}P nuclear spin can be measured using the idea of adiabatic evolution of states. The idea is to transfer the detection of the nuclear spin to the electrons. Suppose that at $J = 0$, $A_1 > A_2$, the energy levels of nuclear spin states in electron spin ground state, $|\downarrow\downarrow\rangle$, are in the following order with $|10\rangle$ above $|01\rangle$ ($|10\rangle$ and $|01\rangle$ are degenerate when $A_1 = A_2$): $|11\rangle$, $|10\rangle$, $|01\rangle$, and $|00\rangle$. This procedure distinguishes energy state of nuclear spin #1 from that of nuclear spin #2. If now J is turned on and increased adiabatically (but still $J < \mu_B B/2$) and at the same time $\Delta A = A_1 - A_2$ is turned off adiabatically, then the $|10\rangle$ and $|01\rangle$ states evolve gradually into $|s_n\rangle$ and $|a_n\rangle$ respectively. The above few steps of operations are similar to the first few steps performed in the controlled-NOT procedure described in Sec. VII. If J is increased further adiabatically from $J < \mu_B B/2$ to $J > \mu_B B/2$, according to Fig. 6 or Eq. (60), the system with nuclear spin state in either $|11\rangle$ or $|s_n\rangle$ will remain in the same electron-nuclear state. On the other hand, the electron spin state of the system with nuclear spin state in either $|00\rangle$ or $|a_n\rangle$ will evolve into the $|a_e\rangle$ state. Thus the initial orientation of nuclear spin #1 alone will determine what electron spin state the system evolves into. To be more evident, if initially the system is in the electron spin polarized $|\downarrow\downarrow\rangle$ state and the orientation of nuclear spin #1 is down, i.e., in $|1\rangle$ state, by means of the above sequence of adiabatic steps, no matter what the orientation of the second nuclear spin has, the system will remain in the same electron spin state $|\downarrow\downarrow\rangle$. However, if initially nuclear spin #1 is in $|0\rangle$ state, the electron spin state of the system will evolve into $|a_e\rangle$ state. We summarize the sequence of steps performed and the associated adiabatic evolution of states in the following:

$$\begin{aligned}
&J = 0,\ A_1 > A_2 \qquad 0 < J < \tfrac{\mu_B B}{2},\ \Delta A \gg h\nu_J\\
&|\downarrow\downarrow\rangle|11\rangle \longrightarrow |\downarrow\downarrow\rangle|11\rangle\\
&|\downarrow\downarrow\rangle|10\rangle \longrightarrow |\downarrow\downarrow\rangle|10\rangle\\
&|\downarrow\downarrow\rangle|01\rangle \longrightarrow |\downarrow\downarrow\rangle|01\rangle\\
&|\downarrow\downarrow\rangle|00\rangle \longrightarrow |\downarrow\downarrow\rangle|00\rangle
\end{aligned}$$

$$\begin{aligned}
&0 < J < \tfrac{\mu_B B}{2},\ A_1 = A_2 \qquad J > \tfrac{\mu_B B}{2},\ A_1 = A_2\\
&\longrightarrow\ |\downarrow\downarrow\rangle|11\rangle \longrightarrow |\downarrow\downarrow\rangle|11\rangle,\\
&\longrightarrow\ |\downarrow\downarrow\rangle|s_n\rangle \longrightarrow |\downarrow\downarrow\rangle|s_n\rangle,\\
&\longrightarrow\ |\downarrow\downarrow\rangle|a_n\rangle \longrightarrow |a_e\rangle|11\rangle,\\
&\longrightarrow\ |\downarrow\downarrow\rangle|00\rangle \longrightarrow |a_e\rangle|a_n\rangle.
\end{aligned} \tag{61}$$

From Eq. (61), if the final electron spin states, $|\downarrow\downarrow\rangle$ and $|a_e\rangle$, of the two neighboring donor atom system are, by some means, distinguishable from each other, the initial orientation of nuclear spin #1 can thus be determined.

A method to detect the nuclear and electron spin states using electronic means is shown in Fig. 7. The basic idea is to turn the spin measurement into a charge measurement. Suppose a two-qubit quantum gate operation was just done. These two qubits located right below the A gates in Fig. 7, have no coupling between them and are now ready to be read out (for the purpose of quantum computing, the qubits must be coupled only for the short time of switching, while most of time there is to be no coupling between them). Let us call the other two donor atoms located below the single-electron transistors (SETs) and on the left and right of the two qubits in Fig. 7 the L-donor and R-donor atoms respectively. For the purpose of nuclear spin readout, we take the L-donor and the neighboring first qubit as a system, and the second qubit and its neighboring R-donor atom as the other system. In order to investigate the difference in spin detection between the two possible values of nuclear spin, we

assume that the nuclear spin of one of the two qubits, say the first qubit, is in $|1\rangle$ state and the nuclear spin of the other qubit, say the second qubit, is in $|0\rangle$ state. After the sequence of adiabatic steps stated in Eq. (61) (which can be performed simultaneously for both of the systems), the electron state of the system consisting of the L-donor and first qubit will remain in $|\downarrow\downarrow\rangle$ state, and the electron state of the other system containing the second qubit and the R-donor atom will evolve into $|a_e\rangle$ state, illustrated schematically in Fig. 7 (b). The ^{31}P donor in Si has a stable two-electron state (D^- state) with a second electron binding energy of 1.7meV, but only if the relative spin of the two electrons is a singlet. Therefore even if the A gates above the two qubits are biased appropriately, electron charge motion between the donors will only occur if the electrons are in the singlet $|a_e\rangle$ state. For the above assumed initial values for the two qubits, only the electron on the second qubit (initially in $|0\rangle$ state) will tunnel into R-donor atom forming a D^- state. As a result, a perturbation on the conductance of the highly charge-sensitive SET above the R-donor atom will be observed. On the other hand, no change on the conductance of the SET above the L-donor atom is expected. To sum up, the job of measuring spin is converted into a job of measuring charge movement of electron tunneling into D^- state. If a perturbation signal is observed in the SET, the nuclear spin of the measured qubit is in $|0\rangle$; if the SET does not detect any change in tunneling current, then the measured qubit is in $|1\rangle$.

IX. MEASUREMENT PROCESS AND CONTINUOUS OBSERVATION

In the previous section we saw that the measurement reduces to the problem of monitoring the conductance of the SET while an electron tries to tunnel from the 2nd-qubit to the D^- state of the R-donor. Like all measurement processes the SET induces a non-unitary component to the tunneling dynamics. The tunneling system (from $|a_e\rangle \leftrightarrow |D^-\rangle$ finds itself continuously monitored, and is thus coupled to the irreversible processes in the SET. This kind of system is analyzed in the paper on SET measurements on two couple quantum dots[9]. When one level of a two level system is continuously monitored, attention must be paid to the relative rates of coherent and incoherent processes. In fact if one level is monitored too well, the coherent tunneling into that level can be suppressed entirely, a feature known as the quantum watchdog effect.

The idea of the watchdog effect is quite simple. To see how it works consider a two level system with states $|0\rangle$, $|1\rangle$ coupled by a tunnel coupling rate Ω. If the system starts in the state $|0\rangle$, then in time t it evolves to the sate

$$|\psi(t)\rangle = \cos(\Omega t)|0\rangle + \sin(\Omega t)|1\rangle \qquad (62)$$

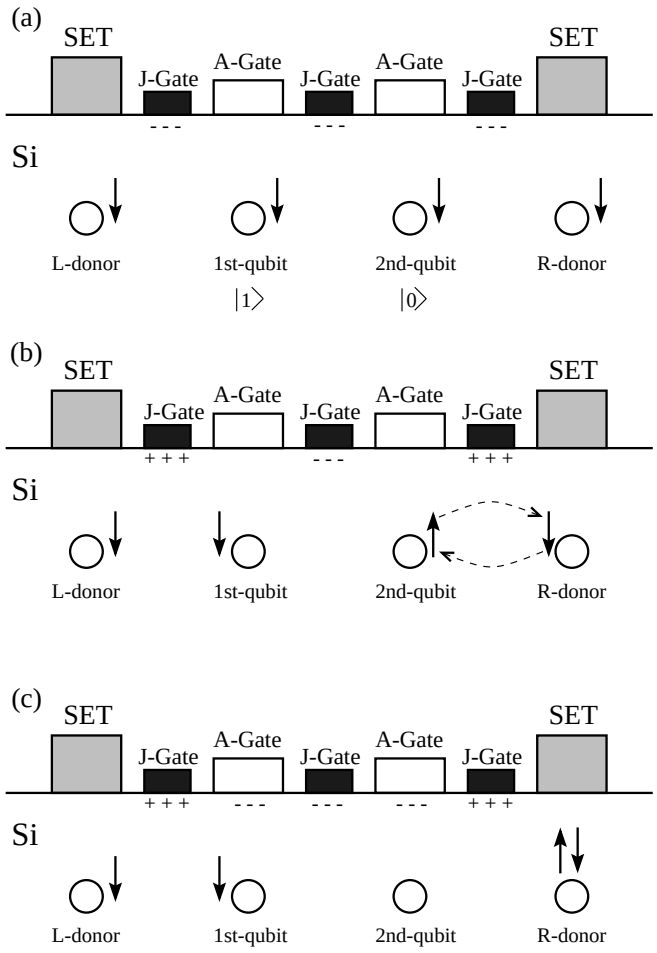

FIG. 7. Schematic illustration of the two-qubit and spin measurement system. (a) The two qubits are initially in nuclear spin $|1\rangle$ and $|0\rangle$ states respectively and all the donor electrons are all in the spin $|\downarrow\rangle$ states. (b) After the sequence of adiabatic process for spin readout stated in Eq. (61), the electron state of the system consisting of the L-donor and first qubit evolves into $|\downarrow\downarrow\rangle$ state, while the electron state of the other system containing the second qubit and the R-donor atom evolves into $|a_e\rangle$ state. (c) By applying appropriate bias of the A gate voltage above the two qubits, only the electrons in $|a_e\rangle$ state in the system consisting of the 2nd qubit and R-donor atom can make transitions into a state in which the two electrons are bound to the same donor (D^- state). The electron current during the transition is measured using highly charge-sensitive SET, enable the underlying spin states of the electron and nuclei to be determined.

Suppose now that a fixed times an instantaneous, perfectly accurate readout (projective readout) is made of state $|1\rangle$, and that these occur with a frequency γ. The time between successive readouts is then $T = 2\pi/\gamma$. The result of each readout is 0 if the system is not found in state $|1\rangle$, otherwise the result is 1. If the result is 0 then consistency demands that immediately after this readout the system state is $|0\rangle$. Suppose now that the system starts in state $|0\rangle$. The probability that we get the null result at the first readout is

$$P_n^{(1)}(T) = \cos^2(\Omega T) \tag{63}$$

which is close to unity if the measurements occur more rapidly then the tunneling period. The probability that we get a null result for the first N readouts up to time $t = NT$ is then

$$P_n^{(N)}(NT) = \cos^{2N}(\Omega T) \tag{64}$$

We now take a continuous limit in which $T \to 0$ and $N \to \infty$ such that $t = NT$ is finite. The probability that at time t we have never seen the system in state $|1\rangle$ that is we have only seen null results) is then just

$$\begin{aligned} P_n(t) &\approx (1 - \frac{\Omega^2 T^2}{2})^N \\ &\approx (1 - \frac{NT\Omega^2 T}{2}) \\ &\approx e^{-\Omega^2 tT/2} \\ &\to 1 \quad \text{as } T \to 0 \end{aligned}$$

The continuous observations have completely overwhelmed the coherent tunneling so that the system NEVER enters the state $|1\rangle$. This is because, for short times, the coherent process goes as t^2 while the incoherent measurement process goes as t. The lesson is that, for continuously monitored tunneling systems, we must treat carefully the nature of the irreversible coupling between the system and the apparatus, and be mindful of the time scales. Such an analysis is undertaken in Ref.[9]. In the case of the SET there is an additional problem associated with the background current though the SET which is shot-noise limited. Even when the SET is not fully on, this background current will decohere the system as it tries to tunnel between the two states. Form the experimental point of view, the effect of the background current is to render the two possible output current states difficult to distinguish and thus a reliable determination of the position of the electron is difficult to make.

X. ADIABATIC SWITCHING

In the proposed quantum gate and measurement operations, the exchange J and hyperfine interaction A are switched on and off adiabatically by the external electric J and A gates respectively. We discuss in this section some issues concerning adiabatic switchings. In a problem with a slowly and continuously varying Hamiltonian $H(t)$, the adiabatic theorem in quantum mechanics states that in the limit of infinitely slow or adiabatic passage, if the system is initially in a eigenstate of $H(0)$, it will, at time t, have passed into the eigenstate of $H(t)$ that derives from it by continuity. In other words, the variation is so slow that the system is able to respond as if the time evolution energy states are determined by the instantaneous eigenstate of the Hamiltonian. Thus for the adiabatic processes to be very accurate, the gate biases have to be swept very slowly, i.e., adiabatic switching time should be as long as possible (but must smaller than the decoherence time). However, for the purpose of quantum computing, the rule for the switching speed is the faster the better as long as the errors introduced in the prescribed manipulations are tolerable by error correction. This issue of adiabaticity has been discussed for quantum gate based on electron spins in coupled quantum dots[7]. We describe below some adiabatic conditions relevant to the silicon-based nuclear spin quantum computer.

The important question to be answered is the following: how slow does the change in the Hamiltonian or in the electric voltage in A and J gates, have to be to allow the adiabatic process to be valid. Adiabatic switchings via an external control field $v(t)$ (electric voltage in A or J gates, for example) require at least

$$\left|\frac{\dot{v}(t)}{v(t)}\right| \ll \frac{\delta\varepsilon}{\hbar}, \tag{65}$$

where $\delta\varepsilon$ is a characteristic energy scale of the problem. Since the qubits are coupled within the switching time, τ_s, a typical frequency scale during switching is then given by the nuclear exchange energy ν_J, (58), for Kane's nuclear spin system in Si while it is the electron exchange $4J/h$ for electron spin system in coupled quantum dots[7]. Adiabaticity requires that many coherent oscillations have to take place between qubits while external control parameters $v(t)$ (electric voltage in A or J gates, for example) is being changed, i.e., $1/\tau_s \approx |\dot{v}(t)/v(t)| \ll \nu_J$. This nuclear spin exchange frequency ν_J hence approximates the rate at which binary operations can be performed on the computer. For $\nu_J \approx 75$KHz, we see that τ_s should not be smaller than about 14μs.

Certain pulse shapes[8] may not be suitable for adiabatic switching. Switching pulses of rectangular shape, for example, are excluded by the adiabaticity requirement. The Fourier transform, $v(\omega)$, for a rectangular pulse $v(t)$ decays only as $1/\omega$, and in this case many excitations into higher energy levels will occur. For a Gaussian pulse shape, we would get $|\dot{v}(t)/v(t)| \propto t$ and some cutting of the long-time tails is required in order to satisfy adiabaticity for all times. An adiabatic pulse shape of amplitude v_0 is, for example, given by

$$v(t) = v_0 \mathrm{sech}(t/\Delta t), \tag{66}$$

where $\Delta t = \tau_s/\beta$ gives the width of the pulse and β is chosen such that $v(\tau_s)/v_0$ becomes vanishingly small. In this case we have

$$\left|\frac{\dot{v}(t)}{v(t)}\right| = \frac{1}{\Delta t}\left|\tanh\left(\frac{t}{\Delta t}\right)\right| \leq \frac{1}{\Delta t} = \frac{\beta}{\tau_s}. \tag{67}$$

Thus for adiabaticity we need to choose τ_s such that $\beta/\tau_s \ll \delta\varepsilon/\hbar$. The Fourier transform,

$$v(\omega) = v_0 \pi \Delta t \,\mathrm{sech}(\pi\omega\Delta t), \tag{68}$$

has the same shape as $v(t)$ but with a width of $2/(\pi\Delta t)$ and it decays exponentially in frequency ω.

The actual pulse shape of the switching may not be very relevant for the quantum gate operation since the only parameter which matters is the integrated pulse shape, $\int_0^{\tau_s} \nu_J(v(t))dt$ for example. Other more efficient operations than the adiabatic approaches are desired.

XI. CONCLUSION

We have exploited the silicon-based electron-mediated nuclear spin quantum computer proposed by Kane. Especially, the single- and two-qubit energy levels and eigen states as well as their operations and measurements are discussed in details. Issues regarding adiabatic procedures, such as adiabatic switching times and pulse shapes are also briefly discussed.

---

[a] E-mail: goan@physics.uq.edu.au.
[b] E-mail: milburn@physics.uq.edu.au.

[1] B. E. Kane, Nature **393** 133 (1998).
[2] B. E. Kane, unpublished.
[3] see, for example, B. Sapoval and C. Hermann, *Physics of Semiconductors* (Springer-Verlag, New York, 1995); P. Y. Yu and M. Cardona, *Fundamentals of Semiconductors* (Springer-Verlag, Berlin, 1996).
[4] R. A. Faulkner, Phys. Rev. **184**, 713 (1969).
[5] S. Pantelides and C. T. Sah, Phys. Rev. B **10**, 621 (1974); ibid. 638 (1974).
[6] K. Andre et. al., Phys. Rev. B **24**, 244 (1981).
[7] D. Loss and D. P. DiVincenzo, Phys. Rev. A **57**, 120 (1998).
[8] D. P. DiVincenzo and D. Loss, e-print cond-mat/9901137.
[9] H. M. Wiseman, Dian Wahyu Utami, He Bi Sun, G. J. Milburn, B. Kane, A. Dzurak and R. Clark, cond-mat/0002279.